A geometric constraint, the head-to-tail exclusion rule, may be the basis for the isolated-pentagon rule in fullerenes with more than 60 vertices

Stan Schein[a,b,c,1] **and Tara Friedrich**[c]

[a]California NanoSystems Institute, [b]Brain Research Institute, and [c]Department of Psychology, University of California, Los Angeles, CA 90095

Edited by Charles F. Stevens, The Salk Institute for Biological Studies, La Jolla, CA, and approved October 27, 2008 (received for review August 2, 2008)

Carbon atoms self-assemble into the famous soccer-ball shaped Buckminsterfullerene (C_{60}), the smallest fullerene cage that obeys the isolated-pentagon rule (IPR). Carbon atoms self-assemble into larger ($n > 60$ vertices) empty cages as well—but only the few that obey the IPR—and at least 1 small fullerene ($n \leq 60$) with adjacent pentagons. Clathrin protein also self-assembles into small fullerene cages with adjacent pentagons, but just a few of those. We asked why carbon atoms and clathrin proteins self-assembled into just those IPR and small cage isomers. In answer, we described a geometric constraint—the head-to-tail exclusion rule—that permits self-assembly of just the following fullerene cages: among the 5,769 possible small cages ($n \leq 60$ vertices) with adjacent pentagons, only 15; the soccer ball ($n = 60$); and among the 216,739 large cages with $60 < n \leq 84$ vertices, only the 50 IPR ones. The last finding was a complete surprise. Here, by showing that the largest permitted fullerene with adjacent pentagons is one with 60 vertices and a ring of interleaved hexagons and pentagon pairs, we prove that for all $n > 60$, the head-to-tail exclusion rule permits only (and all) fullerene cages and nanotubes that obey the IPR. We therefore suggest that self-assembly that obeys the IPR may be explained by the head-to-tail exclusion rule, a geometric constraint.

Buckminsterfullerene | buckyball | self assembly | clathrin

Fullerenes are closed cages with an even number $n \geq 20$ of three-connected vertices, $3n/2$ edges, 12 pentagonal faces, and $(n\text{-}20)/2$ hexagonal faces (1, 2). The soccer ball with $n = 60$ vertices is the smallest fullerene with all of its pentagons surrounded ("isolated") by hexagons. It is therefore said to obey the "isolated-pentagon rule" (IPR) (2–5). No cage that obeys the IPR is mathematically possible for $62 \leq n \leq 68$, but IPR cage isomers are possible for every even $n \geq 70$, the number generally growing as n grows (2). In accord with the IPR, carbon atoms self-assemble into the soccer-ball shaped Buckminsterfullerene (C_{60}) (1) and larger fullerene cages, but only those few that obey the IPR, starting with the one IPR isomer of C_{70} (Fig. 1*A*) (6–9).

Various explanations have been offered for the IPR. Kroto suggested that "strain-related instability" within the network of σ bonds was minimal for cages with isolated pentagons but increased with pairs of adjacent pentagons, even more so with clusters of 3 pentagons, etc (3). Schmalz and colleagues offered a quite different explanation, that adjacent pentagons had "eight-cycles," in violation of Hückel's $4n + 2$ rule, thus focusing on diminution of π bond interaction by adjacent pentagons (4, 5). Later, because π orbital overlap is also reduced generally by cage curvature (10, 11), they suggested that overlap would be most greatly reduced at the sites of greater (and anisotropic) curvature produced by adjacent pentagons (12). These mechanisms work together for Buckminsterfullerene but not necessarily for larger IPR cages and not for smaller cages with adjacent pentagons, at least 1 of which is also formed by carbon (13, 14).

Here, we propose an alternate explanation for the IPR. Initially focusing on the small fullerene cages ($n \leq 60$ vertices) with adjacent pentagons into which the protein clathrin (15) and carbon atoms self-assemble (13, 14) [e.g., 36-15 (the 15th isomer with 36 vertices) and 28-2 (the 2nd isomer with 28 vertices)], we described a geometric constraint, the head-to-tail exclusion rule (16, 17). Among the 5769 small cages with adjacent pentagons, the head-to-tail exclusion rule permits self-assembly of just 15. It also permits self-assembly of the IPR soccer ball ($n = 60$).

When we investigated larger cages in the range $60 < n \leq 84$, we were surprised to discover that the head-to-tail exclusion rule permits only (and all of) the 50 cages that obey the IPR in this range of n. Might it permit some larger non-IPR fullerene? There is precedent for such a concern; for example, the pentagon-spiral algorithm (18) produces every 1 of >1 million fullerene cage isomers before missing one with 100 vertices (19, 20). To be regarded as an explanation for the IPR, the head-to-tail exclusion rule would have to be shown to permit only and all IPR cages for *all* $n > 60$. Here, by proving that the largest permitted cage with adjacent pentagons is one with $n = 60$ vertices, we do so. In addition, based on the physical mechanism underlying the operation of the head-to-tail exclusion rule (17), that the head to tail rule identifies fullerenes with severely nonplanar faces that are unlikely to self-assemble and are energetically disfavored, we describe how the head-to-tail exclusion rule promotes production of IPR cages.

Model

Dihedral Angle Discrepancy (DAD). The head-to-tail exclusion rule relies on appreciation of "dihedral angle discrepancy" (DAD) (16). As shown in Fig. 1*B*, a DAD is a vector that we draw along an edge that abuts a pentagon at one end and a hexagon at the other. Depending on the faces to the sides of the edge, we color the DAD "green" (two side hexagons), "red" (a hexagon and a pentagon), or "blue" (two pentagons). The dihedral angles about an edge with a green DAD are 138.2° at its pentagon end and 180° at its hexagon end, so the green DAD corresponds physically to an increase (or broadening) of dihedral angle of 41.8° (17). This broadening requires that one or usually both of the faces on either side of such an edge—the two hexagons marked with asterisks in Fig. 1*B* in the case of a green DAD—cannot be planar.

In the three-dimensional IPR 70 fullerene cage shown in Fig. 1*A*, we mark just one green DAD, with its tail at the pentagon end of the edge and its head at the hexagon end. In the corresponding two-dimensional "Schlegel diagram" representation shown in Fig. 1*C*, we mark all 20 of the green DADs. In Fig. 1*A*, the nonplanar side faces (hexagons) are evident along the cinched "waist" of the IPR 70 cage.

Edges with "red" and "blue" DADs have adjacent pentagons

Author contributions: S.S. and T.F. designed research, performed research, analyzed data, and wrote the paper.

The authors declare no conflict of interest.

This article is a PNAS Direct Submission.

[1]To whom correspondence should be addressed. E-mail: schein@ucla.edu.

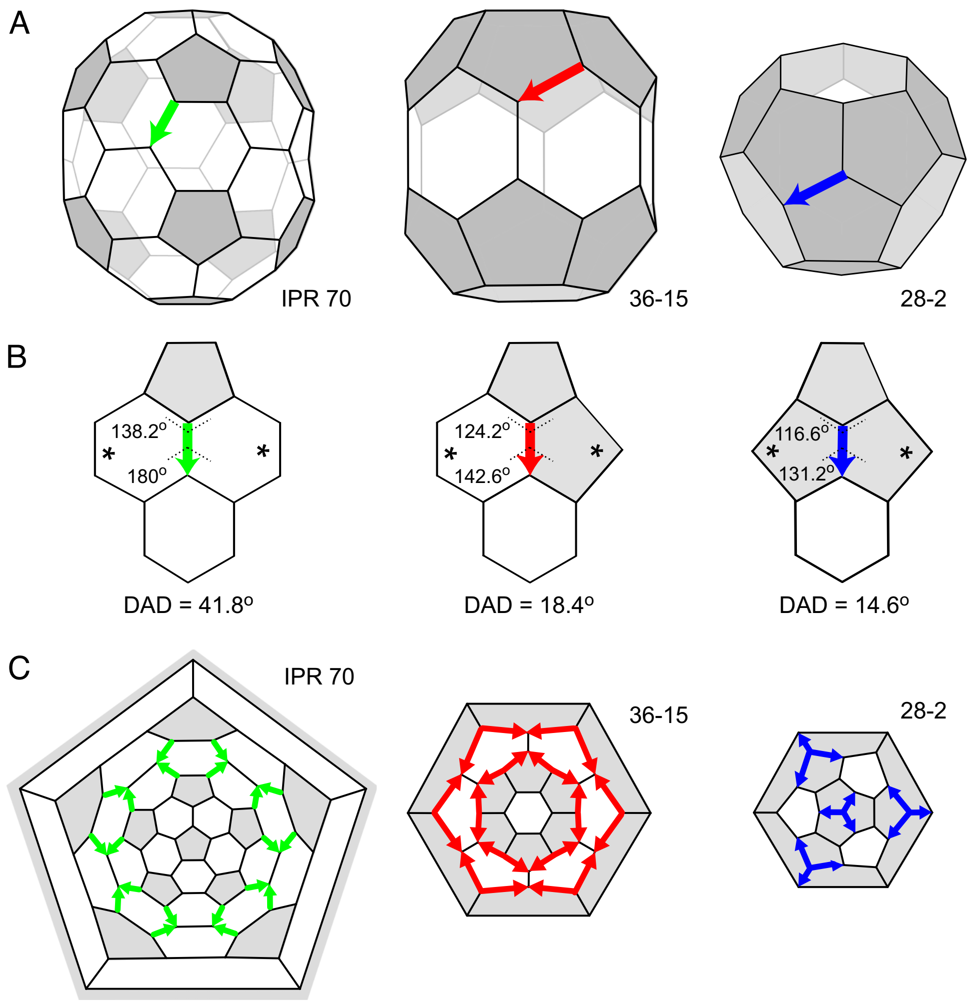

Fig. 1. Almost all fullerene cages have edges with dihedral angle discrepancy (DAD) and thus some nonplanar faces. (*A*) An IPR fullerene cage (IPR 70) and two small cages (36–15 and 28–2) with adjacent pentagons, the first 2 self-assembled by carbon atoms, the last 2 by clathrin. Just one DAD is drawn in each cage. (*B*) When the faces at the two ends of an edge are different, the dihedral angle about that edge at its hexagon end is broader than the dihedral angle about that edge at its pentagon end, establishing a dihedral angle discrepancy (DAD). With two faces (marked by asterisks) to the side of such an edge that are both hexagons (green DAD), or 1 hexagon and 1 pentagon (red DAD), or 2 pentagons (blue DAD), the magnitudes of the dihedral angles at the two ends of these colored edges are different, and the magnitudes of the DADs are different (41.8°, 18.4°, and 14.6°, respectively). (*C*) Each of the Schlegel diagrams of the cages selected for part A shows many DADs: 20 green ones for the IPR 70 cage, 24 red ones for the 36–15 cage, and 12 blue ones for the 28–2 cage.

(Fig. 1*B*). We mark a red DAD (Fig. 1*B*) in the 36–15 fullerene cage (Fig. 1*A*) and all 24 red DADs in the corresponding Schlegel diagram (Fig. 1*C*). The nonplanar side hexagons are also visibly nonplanar along the cinched waist of 36–15 in Fig. 1*A*. (The nonplanar side pentagons cannot be appreciated from this figure.) We mark a blue DAD (Fig. 1*B*) in the 28–15 fullerene cage (Fig. 1*A*) and all 12 blue DADs in the corresponding Schlegel diagram (Fig. 1*C*).

The dodecahedron ($n = 20$) has only one type of vertex, pentagon-pentagon-pentagon, and thus no DADs. The soccer ball ($n = 60$) has only one type of vertex, pentagon-hexagon-hexagon, and thus no DADs as well. All other fullerene cages—including IPR ones—have more than one type of vertex, thus some edges with a DAD, and thus some nonplanar faces (16). For this reason, although from the point of view of graph theory fullerene cages are described as convex polyhedra, from the point of view of solid geometry they are generally neither convex nor polyhedra (with exclusively planar faces). The existence of these other fullerene cages, like the ones in Fig. 1*A* for carbon (IPR 70 and 36–15) and for clathrin (36–15 and 28–2), proves that the presence of nonplanar faces does not necessarily exclude self-assembly of a fullerene.

Rings. The nature—DAD or no DAD—of all of the edges of a face can be assigned if the identities—pentagons and hexagons—of all of its surrounding faces are known. We call such arrangements Rings. Fig. 2*A* shows all 8 pentagon-centered Rings ("pent-Rings") and all 13 hexagon-centered Rings ("hex-Rings") from (16). In a fullerene cage, every pentagonal face can be regarded as the central face of a pent-Ring, and every hexagonal face can be regarded as the central face of a hex-Ring. We can therefore label every pentagon or hexagon with its pent-Ring type (e.g., 521) or hex-Ring type (e.g., 611). As can be seen in Fig. 2*A*, the edges of the central face of a Ring can have 0, 2, or 4 DADs. What is new in Fig. 2*A* is how the Rings are grouped for the purpose of this article's proof, a critical advance over the corresponding figure in ref. 16.

Head-to-Tail Exclusion Rule. As noted above, most of the different fullerenes that have been isolated and identified have DADs and thus nonplanar faces (e.g., Fig. 1). The head-to-tail exclusion rule specifically excludes just the Rings that have DADs arranged head-to-tail, namely, the 2 pent-Rings (521 and 531) and 4 hex-Rings (621, 631, 632, and 642) grouped together in Fig. 2*A Left*.

Fig. 2*B* illustrates the physical basis for the head-to-tail exclusion rule. Edges *c* and *a* in that figure are examples of "external edges" because they are external to the central face of a Ring, and edge *b* is an example of a "central edge" because it is an edge of the central face. "External rotation" refers to the rotation (in a surrounding face of a Ring) of external edges from one another, for example, edge *c* from external edge *a* about central edge *b*. In Rings with head-to-tail DADs, the magnitude of the external rotation about a central edge with DAD is equal to nearly the entire DAD about that edge, for example, 41.8° for an edge with a green DAD, and the resulting nonplanarity of the surround face is very severe. In Rings without head-to-tail

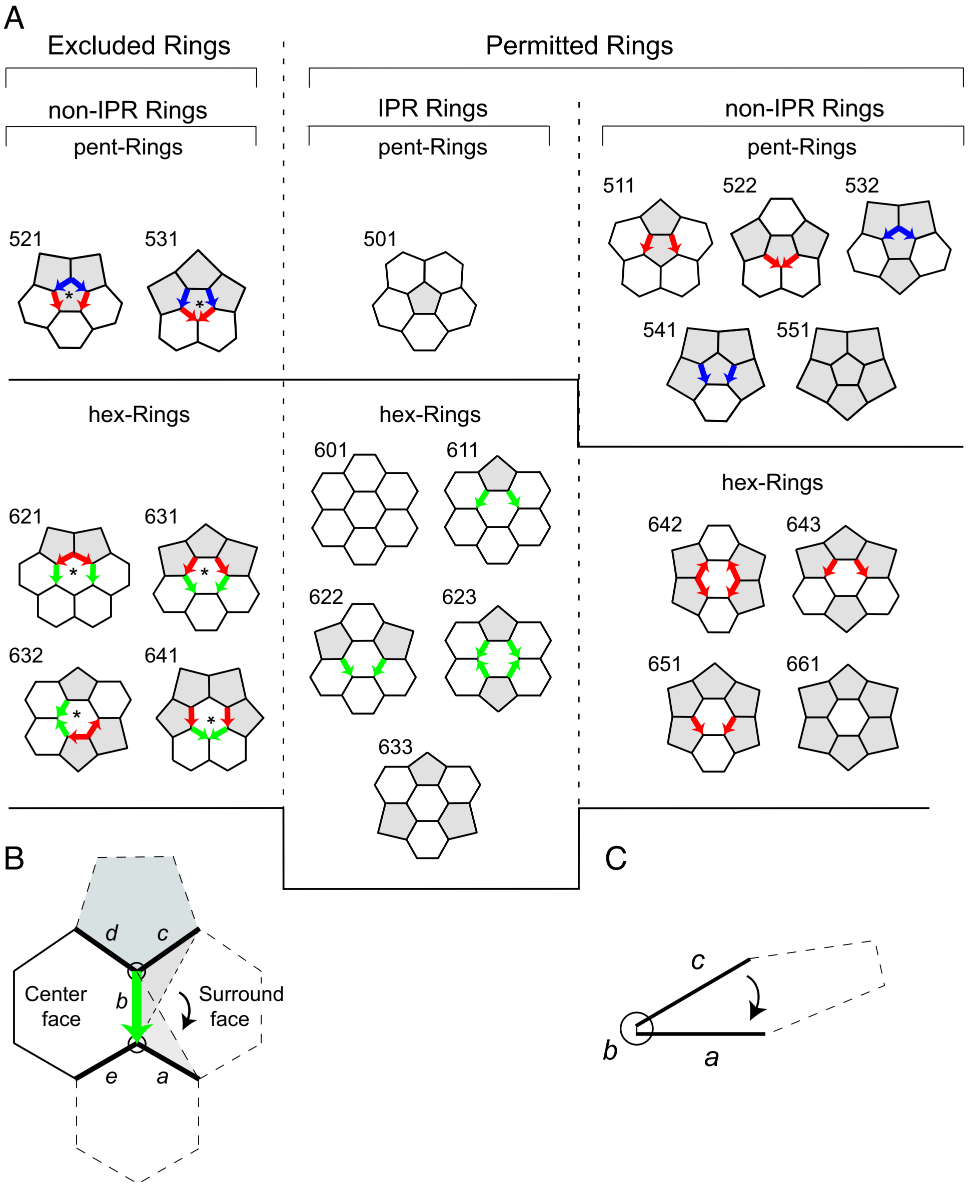

Fig. 2. Rings may be grouped according to their arrangements of edges with DAD. (*A*) Each pent-Ring (or hex-Ring) has a particular arrangement of the 5 (or 6) faces surrounding a pentagon (or a hexagon). These may be grouped as follows: the *Left* has Rings with head-to-tail DADs, all excluded; the *Middle* has permitted Rings with no adjacent pentagons, thus IPR; the *Right* has permitted Rings with adjacent pentagons, thus non-IPR. (*B*) A DAD like a green one in hex-Ring 611 or in hex-Ring 631 produces rotation of edge *a* (external to the central face) from edge *c* (also external to the central face) about the green central edge (*b*), more so for a Ring with head-to-tail DADs (e.g., 631). This ''external rotation'' of edge *a* from edge *c* is equal to the (dihedral) angle between the two shaded planes in the surround face. (*C*) Sighting down edge *b* in *B* shows clearly this external rotation and the resultant nonplanarity of a surrounding face that would contain edges *a* and *c*.

DADs, the external rotation due to the DAD is shared among surrounding faces, and the resulting nonplanarity of the surrounding faces is much less severe (17).

Fig. 2*C*, the result of sighting down edge *b* in Fig. 2*B*, permits appreciation of the severely nonplanar surrounding face external to a green DAD edge in one of the excluded Rings (hex-Ring 631). In such excluded Rings, several of the surrounding faces would be severely nonplanar, a geometry (or energy cost) that would make self-assembly (or persistence) of excluded Rings highly improbable (or fleeting) (17).

Cages Permitted by the Head-to-Tail Exclusion Rule. Correspondingly, self-assembly of mathematically possible fullerene cage isomers that contained excluded Rings would be improbable. After excluding all such improbable cages for $20 \le n \le 84$, the head-to-tail exclusion rule permits only the 15 "small" ($n \le 60$) fullerene cages with adjacent pentagons shown in Fig. 3, the IPR soccer ball ($n = 60$), and only and all of the IPR cages for $60 < n \le 84$ (16). It permits no cage for $60 < n \le 84$ with adjacent pentagons. In the whole range studied, $20 \le n \le 84$, the largest permitted cage with adjacent pentagons is 60–1784 (Fig. 3). Because we follow *An Atlas of Fullerenes* (2) in numbering isomers (e.g., isomer 1784 with 60 vertices), the highest numbered isomers have the most dispersed pentagons. With 1812 isomers for $n = 60$, isomer 1784 is close to having the most dispersed isomers, but 60–1812—the soccer ball—wins that distinction.

Results

First, we review why the head-to-tail exclusion rule permits any fullerene cage that is IPR. Then we prove that the largest permitted cage with adjacent pentagons is 60–1784, thus showing that the head-to-tail rule permits *only* as well as *all* IPR cages for *all* $n > 60$, not just for $60 < n \le 84$.

All IPR Cages Are Permitted. By definition, an "isolated" pentagon has no adjacent pentagons. Fig. 2*A Middle* groups together all of the Rings that have no adjacent pentagons, that is, "IPR Rings." There is just one IPR pent-Ring (501), but there are 5 IPR hex-Rings (601, 611, 622, 623, and 633). Therefore, IPR cages can contain only the 501 type of pent-Ring, a pentagon surrounded by 5 hexagons, and these 5 types of hex-Ring. None of

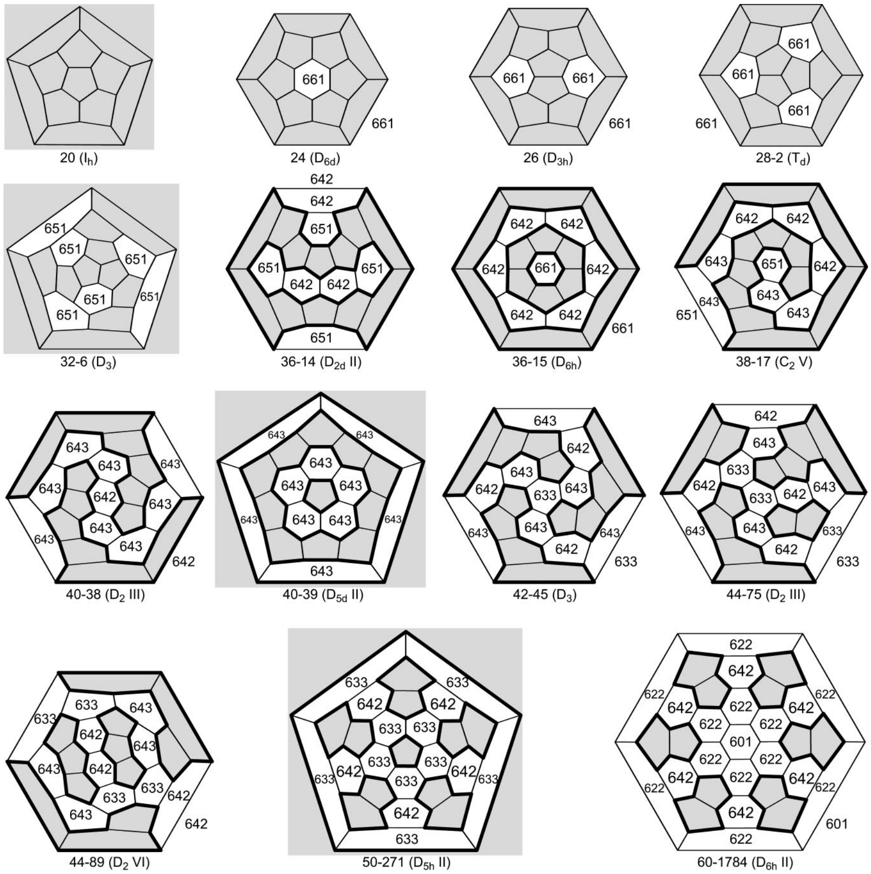

Fig. 3. For fullerenes with $20 \leq n \leq 60$ vertices, the head-to-tail exclusion rule permits only these 15 isomers with adjacent pentagons and the IPR soccer ball (data not shown). The isomers are represented by Schlegel diagrams produced by the Carbon Generator (CaGe) program (available at www.mathematik.uni-bielefeld.de/~CaGe) (36). For any given *n* (e.g., 50 vertices), isomers are specified by number—the highest numbered one (e.g., the 271st isomer, thus 50–271) having the most dispersed pentagons (2)—and also by symmetry point group (e.g., D_{5h}). Hex-Rings are numbered as in Fig. 2*A*. Strings and rings of pentagons are outlined by thick edges.

these Rings have head-to-tail DADs; therefore, none of these IPR Rings are excluded by the head-to-tail exclusion rule; therefore, all IPR fullerenes are permitted (16).

60–1784 Is the Largest Permitted Cage with Adjacent Pentagons. ***Permitted non-IPR Rings.*** Fig. 2*A Right* groups together all of the permitted pent-Rings with adjacent pentagons (511, 522, 532, 541, and 551) and all of the permitted hex-Rings with adjacent pentagons (642, 643, 651, and 661). Of particular note, each of the central hexagons in the latter non-IPR hex-Rings "anneals" surrounding pentagons on one side of the Ring to pentagons on the other side, thus limiting dispersal of pentagons. For example, among its surrounding faces, hex-Ring 642 has 2 pentagons on one side and 2 pentagons on the other side. Without the second set of pentagons, the hexagon would have been hex-Ring 621 (Fig. 2*A Left*), which has head-to-tail DADs and would be excluded.

Pentagon doublets. We showed that among fullerenes with $20 \leq n \leq 84$ the largest permitted cage with adjacent pentagons is 60–1784, which has 6 pentagon "doublets" (Fig. 3). As just noted, a hexagon with just one doublet in its surround would be a hex-Ring 621, one of the excluded Rings with head-to-tail DADs. Therefore, the doublets must be paired, as in the surround of hex-Ring 642 (Fig. 2*A Right*). Because no doublets can be left unpaired, the 6 doublets in 60–1784 must be arranged in sequence in a ring with 6 interleaved hexagons, each of them a hex-Ring 642, as marked for 60–1784 in Fig. 3.

IPR cages can reach any size because each pentagon is surrounded ("isolated") by 6—or more—hexagons. Thus, it could be supposed that a cage with 5 pentagon doublets and 2 isolated pentagons might be larger than 60–1784. In fact, that cage is 50–271 in Fig. 3, a smaller cage. That cage has 5 pentagon doublets arranged in sequence in a ring with 5 interleaved hexagons, each of them a hex-ring 642, similar to the arrangement in 60–1784. However, cage 50–271 is smaller than 60–1784 because the ring of 5 pentagon doublets is smaller than the ring of 6.

A hypothetical cage with a ring of fewer than 5 pentagon doublets would be even smaller, but in any case, no such rings of doublets are possible because fullerenes cannot have square or triangular faces, around which such a smaller Ring of 4 or 3 pentagon doublets could be arranged.

Longer linear strings, Rings, and cycles of pentagons. A linear string of 3 hexagons is present in 44–89 (Fig. 3). Hex-Ring 631 in Fig. 2*A Left* has a linear triplet of pentagons in its surround but is excluded by virtue of its head-to-tail arrangements of DADs. Therefore, to avoid head-to-tail DADs, a permitted hexagon with a linear triplet of pentagons in its surround must have additional pentagons in its surround. One such permitted hex-Ring, 643 in Fig. 2*A Right*, contacts a 4th pentagon opposite the linear triplet of pentagons. As a result, the hexagons that line a linear string of 3 pentagons in cage 44–89 (Fig. 3) are a combination of the 642- and 643-types of hex-Ring. The strings of pentagons are thus kept close to one another by the "annealing" hexagons, the result being a small—just 44 vertices—cage.

Similarly, in Fig. 3, hex-Rings 642 and 643 anneal linear strings of 4 pentagons (42–45 and 44–75), 6 pentagons (40–38), and 12

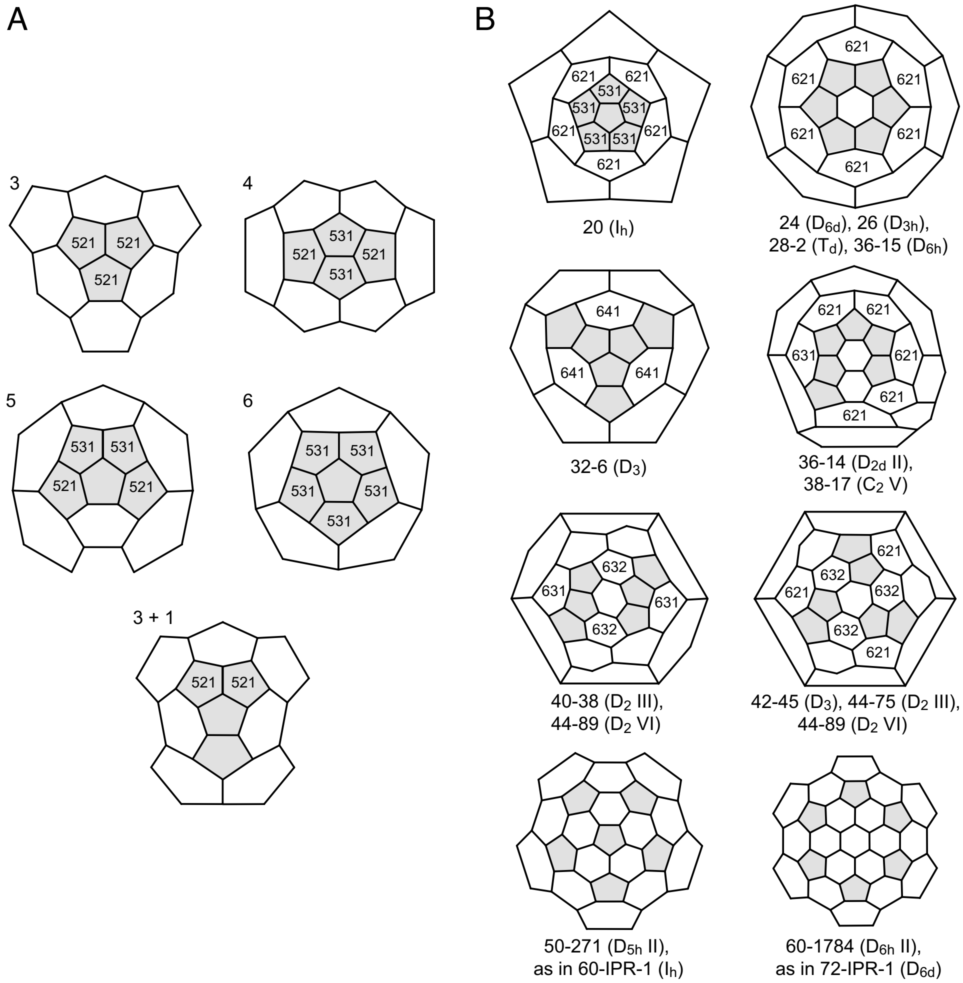

Fig. 4. Independent clusters of pentagons and nanotubes with non-IPR caps are excluded by the head-to-tail exclusion rule. (*A*) In these independent clusters, only pentagons of an excluded type are labeled. In larger cages, clusters would be surrounded by hexagons, and the pentagons at the interface would be an excluded type of pent-Ring, as shown by the labeled faces. Adding a pentagon to a cluster of 3 (3 + 1 in Fig. 4) produces 2 permitted pent-Rings but leaves 2 excluded pent-Rings (labeled) at the top of the cluster. Addition of more pentagons to the cluster could eliminate all of the excluded pent-Rings, but the resulting cage (28–2 or 32–6 in Fig. 3) would be very small. (*B*) In these nanotube caps, only faces of an excluded type of ring are labeled. Caps (containing 6 pentagons) are taken from all of the permitted cages with adjacent pentagons in Fig. 3. With two exceptions, encircling each cap by a ring of hexagons is enough to show excluded pent-Rings and excluded hex-Rings. The two ''exceptions'' are the caps from cage 50-271 and cage 60-1784, which have no adjacent pentagons and thus obey the IPR.

pentagons (to itself) (38–17), linear rings of 6 pentagons (36–15) and 10 pentagons (40–39), and a linear cycle of 12 pentagons (to itself) (36–14). With arrangements of pentagons longer than a doublet, all of these cages have < 60 vertices.

Pentagon clusters. Extended clusters of pentagons are found in very small ($n \leq 32$) permitted cages, but there are no independent clusters (e.g., 3 pentagons) in any of the permitted cages (Fig. 3). Moreover, in larger cages, independent clusters would be surrounded by hexagons, and the pentagons at the interface would be excluded pent-Rings 521 or 531 (Fig. 4*A*).

Nanotubes with Non-IPR Caps. Proof that the largest fullerene with adjacent pentagons permitted by the head-to-tail exclusion rule is 60–1784 also means that the caps on nanotubes must be IPR. The most likely challenge to this claim would come from the caps extracted from the permitted small fullerenes in Fig. 3, a cap being defined as a region with 6 pentagons. However, we need only to add a single additional ring of hexagons—the very beginning of the tube portion of the nanotube—at the circumference of each cap to demonstrate excluded rings (Fig. 4*B*). Moreover, two exceptions prove the rule: The cap from cage 50-271 is IPR; it is also the pentagon-centered half of the IPR soccer ball and IPR nanotubes with caps composed of half of a Buckminsterfullerene cage. The cap from cage 60-1784 is IPR as well; it is also the hexagon-centered half of the one IPR cage with 72 vertices and corresponding nanotubes. Thus, only nanotube caps that obey the IPR are permitted by the head-to-tail exclusion rule.

Discussion

By exhaustive examination of the 216,739 large cages with $60 < n \leq 84$ vertices, we had shown that the geometric constraint embodied by the head-to-tail exclusion rule permitted only the 50 IPR fullerenes for this range of n (16). Here, we have shown why and proven that for *all even* $n > 60$, the head-to-tail exclusion rule permits only and all IPR cages. Therefore, we suggest that the head-to-tail exclusion rule could (and does) explain the isolated pentagon rule (IPR). In addition, the head-to-tail exclusion rule—but not the isolated-pentagon rule—permits self-assembly of the small group of small fullerene cages with adjacent pentagons shown in Fig. 3. One such carbon cage, C_{36}-15, has already been isolated and identified (13, 14), and some assembly conditions have favored unspecified carbon cages with 32, 44 and 50 carbon atoms (21, 22), numbers of vertices represented among the small permitted cages in Fig. 3.

The IPR itself does not allow cages with < 60 vertices, cages that necessarily have adjacent pentagons. Nonetheless, the originators of the IPR (3–5) pointed out that 2 isomers with 50 carbons (50–270 and 50–271) were special in having no adjacent-pentagon configurations larger than a doublet. This line of thinking was formalized by the suggestion that for *every* even n without IPR cages, that is, in the ranges $20 \leq n \leq 58$ and $62 \leq n \leq 68$, favored isomers could be identified as those with fewest pentagon neighbors (2). Likewise, it would be possible to identify lowest-energy isomers for any n, perhaps by measuring curvature energy (23), and likely produce the same list of fewest-pentagon-neighbor isomers.

By contrast, the head-to-tail exclusion rule permits isomers with adjacent pentagons, but only a subset of n, the ones shown in Fig. 3. It permits no isomers with 30, 34, 46, and 48 vertices, and of particular note, no isomers with 52–58 and 62–68 vertices.

Indeed, we have proposed that the abundance of C_{60} could be due to these large gaps on *both* sides of $n = 60$, gaps that leave no nearby smaller or larger cages into which assembly could settle (16). (Similarly, the abundance of the IPR C_{70}, second only to C_{60}, may be related to the gap from 62 to 68.) Thus, the head-to-tail exclusion rule explains not only the IPR but also why Buckminsterfullerene is the most abundant of the IPR carbon fullerenes.

Prior models for IPR fullerene production, including the Pentagon Road (24, 25), the Hexagon Road (26), and fusion of large carbon cycles (27–29), invoke cage growth and internal reorganization to eliminate pentagon adjacencies (30). Together, these processes are supposed to come to an end when a stable structure like Buckminsterfullerene or larger IPR cage is reached (31). Based on the head-to-tail exclusion rule, we proposed the "Probable Road": Carbon atoms would more probably complete Rings with planar faces or Rings with modest nonplanarity than the excluded Rings with head-to-tail DADs, the severely nonplanar ones (16). We have now shown that the only large fullerenes that could self-assemble, those with none of the excluded Rings, would be the IPR ones.

We suppose that 4 mechanisms could contribute to the operation of the Probable Road. As suggested by Fig. 2*C*, 2 carbon atoms would be unlikely to bridge the gap between the ends of edge *c* and edge *a* in an excluded hex-Ring, and 1 carbon atom would be unlikely to bridge the gap between such disparate ends in an excluded pent-Ring. Such a kinetic barrier could operate during growth (*i*) and reorganization (*ii*). In addition, higher order (resonant and double) bonds, which enforce planarity, tend to point away from pentagons (32–35) and thus locate along edges with a DAD (e.g., edge *b* in Fig. 2*B*). The severe rotation out of planarity of edges *c* from *a* about edge *b* in Fig. 2*B* would thus incur a high energy cost. Such a thermodynamic barrier could also operate during both growth (*iii*) and reorganization (*iv*).

1. Kroto HW, Heath JR, O'Brien SC, Curl RF, Smalley RE (1985) C_{60}: Buckminsterfullerene. *Nature* 318:162–163.
2. Fowler DW, Manolopoulos DE (1995) *An Atlas of Fullerenes* (Clarendon, Oxford).
3. Kroto HW (1987) The Stability of the fullerenes C_n (n = 24, 28, 32, 50, 60 and 70). *Nature* 329:529–531.
4. Schmalz TG, Seitz WA, Klein DJ, Hite GE (1986) C_{60} carbon cages. *Chem Phys Lett* 130:203–207.
5. Schmalz TG, Seitz WA, Klein DJ, Hite GE (1988) Elemental carbon cages. *J Amer Chem Soc* 110:1113–1127.
6. Taylor R, Hare JP, Abdul-Sada AK, Kroto HW (1990) Isolation, separation and characterisation of the fullerenes C_{60} and C_{70}: The third form of carbon. *J Chem Soc Chem Commun* 1990:1423–1425.
7. Kikuchi K, *et al.* (1992) Isolation and identification of fullerene family: C_{76}, C_{78}, C_{82}, C_{84}, C_{90} and C_{96}. *Chem Phys Lett* 180:177–180.
8. Thilgen C, Diederich F (2006) Structural aspects of fullerene chemistry—a journey through fullerene chirality. *Chem Rev* 106:5049–5135.
9. Dresselhaus M, Dresselhaus G, Avouris P, eds (2000) *Carbon Nanotubes: Synthesis, Structure, Properties and Applications* (Springer, Berlin).
10. Haddon RC (1987) Pyramidalization: Geometrical interpretation of the π-orbital axis vector in three dimensions. *J Phys Chem* 91:3719–3720.
11. Haddon RC (1993) RC Chemistry of the fullerenes: The manifestation of strain in a class of continuous aromatic molecules. *Science* 261:545–1550.
12. Schmalz TJ, Klein DJ (1993) Fullerene structures. *Buckminsterfullerenes*, eds Billups WE, Ciufolini MA (Wiley, New York), pp 83–102.
13. Piskoti C, Yarger J, Zettl A (1998) C_{36}, a new carbon solid. *Nature* 393:771–774.
14. Fowler PW, Mitchell D, Zerbetto F (1999) C_{36}: The best fullerene for covalent bonding. *J Am Chem Soc* 121:3218–3219.
15. Crowther RA, Finch JT, Pearse BMF (1976) On the structure of coated vesicles. *J Mol Biol* 103:785–798.
16. Schein S, Sands-Kidner M (2008) A geometric principle may guide self assembly of fullerene cages from clathrin triskelia and from carbon atoms. *Biophys J* 94:958–976.
17. Schein S, Sands-Kidner M, Friedrich T (2008) The physical basis for the head-to-tail rule that excludes most fullerene cages from self assembly. *Biophys J* 94:938–957.
18. Manolopoulos DE, May JC, Down SE (1991) Theoretical studies of the fullerenes: C_{34} to C_{70}. *Chem Phys Lett* 181:105–111.
19. Manolopoulos DE, Fowler PW (1993) A fullerene without a spiral. *Chem Phys Lett* 204:1–7.
20. Brinkmann G, Dress AWM (1997) A constructive enumeration of fullerenes. *J Algor* 23:345–358.
21. Handschuh H, Ganteför G, Kessler B, Bechthold PS, Eberhardt W (1995) Stable configurations of carbon clusters: Chains, rings, and fullerenes. *Phys Rev Lett* 74:1095–1098.
22. Kietzman H, Rochow R, Ganteför G, Eberhardt W, Vietze K, Seifert G, Fowler PW (1998) Electronic structure of small fullerenes: Evidence for the high stability of C_{32}. *Phys Rev Lett* 81:5378–5381.
23. Bowick MJ, Nelson DR, Shin H (2007) Interstitial fractionalization and spherical crystallography. *Phys Chem Chem Phys* 9:6304–6312.
24. Heath JR, O'Brien SC, Curl RF, Kroto HW, Smalley RE (1987) Carbon condensation. *Comments Cond Matter Phys* 13:119–141.
25. Smalley RE (1992) Self-assembly of the fullerenes. *Acc Chem Res* 25:98–105.
26. Heath JR (1991) Synthesis of C_{60} from small carbon clusters: A model based on experiment and theory. *Fullerenes: Synthesis, Properties, and Chemistry of Large Carbon Clusters* (American Chemical Society Symposium Serial no. 481), eds Hammond GS, Kuck VJ (Am Chem Soc, Washington, DC), pp 1–23.
27. Wakabayashi T, Achiba Y (1992) A model for the C_{60} and C_{70} growth mechanism. *Chem Phys Lett* 190:465–468.
28. McElvany SW, Ross MM, Goroff NS, Diederich R (1993) Cyclocarbon coalescence: Mechanisms for tailor-made fullerene formation. *Science* 259:1594–1596.
29. Von Helden G, Gotts NG, Bowers MT (1993) Experimental evidence for the formation of fullerenes by collisional heating of carbon rings in the gas phase. *Nature* 363:60–63.
30. Stone AJ, Wales DJ (1986) Theoretical studies of icosahedral C_{60} and some related species. *Chem Phys Lett* 128:501–503.
31. Curl RF (1993) On the formation of the fullerenes. *The Fullerenes: New Horizons for the Chemistry, Physics and Astrophysics of Carbon*, eds Kroto HW, Walton DRM (Cambridge U Press, Cambridge), pp 19–32.
32. Ozaki M, Takahashi A (1986) On electronic states and bond lengths of the truncated icosahedral C_{60} molecule. *Chem Phys Lett* 127:242–244.
33. Disch RL, Schulman JM (1986) On symmetrical clusters of carbon atoms: C_{60}. *Chem Phys Lett* 125:465–466.
34. Taylor R (1993) C_{60}, C_{70}, C_{76}, C_{78} and C_{84}: Numbering, π-bond order calculations and addition pattern considerations *J Chem Soc Perkin Trans* 2:813–824.
35. Bühl M, Hirsch A (2001) Spherical aromaticity of fullerenes. *Chem Rev* 101:1153–1183.
36. Brinkmann G, Friedrichs OD, Dress A, Harmuth T (1997) CaGe—a virtual environment for studying some special classes of large molecules. *Match* 36:233–237.